ELSEVIER

European Journal of Mechanics B/Fluids 21 (2002) 247–263

EUROPEAN JOURNAL OF MECHANICS B/FLUIDS

Analysis of parametric resonance in magnetohydrodynamics

A.D. Sneyd

University of Waikato, Hamilton, New Zealand

Received 15 January 2001; received in revised form 5 September 2001; accepted 17 October 2001

Abstract

Alternating or rotating magnetic fields are often used to stir, shape and support masses of liquid metal. The periodic electromagnetic force may parametrically excite growing disturbances which can be beneficial or detrimental to the process, and the aim of this paper is to develop the analysis of such effects. In many cases parametric excitation is described by a system of coupled simple harmonic oscillators with small periodic forcing and damping terms, and we use Floquet theory to derive a recursion formula for a matrix whose eigenvalues determine the growth rates. We consider two applications in detail – low-frequency magnetic stirring in a circular tank and the instability of a free-surface in the presence of an alternating field.

Keywords: Magnetohydrodynamics; Parametric resonance; Mathieu equation

1. Introduction

In 1831 Faraday observed that when a container of liquid is subjected to vertical vibrations, standing waves may appear on the free surface with a frequency half that of the container [2]. The liquid surface is initially plane, and waves are excited only when the vibration amplitude exceeds a critical threshold depending on the frequency. It can be shown [3] that the amplitude $a(t)$ of each gravity-wave mode of frequency Ω evolves according to Mathieu's equation

$$\ddot{a} + \Omega^2 a + \varepsilon \sin(\omega t) a = 0,$$

where ε is the amplitude and ω the frequency of the applied oscillation. For certain values of the parameters ω and ε (typically when Ω is close to $\frac{1}{2}\omega$) $a(t)$ may grow exponentially with time. The instability regions in the (ω, ε)-plane are well documented [4]. When viscous damping in the boundary layers on the container walls is taken into account one obtains a coupled system of mode evolution equations with convolution operators [5].

The magnetohydrodynamic (MHD) counterpart of the Faraday experiment uses an electrically-conducting liquid (mercury) with periodic forcing provided by a vertical alternating magnetic field [6]. When the field is relatively weak a pattern of concentric waves is excited on the free surface, but as the field intensity increases there is a symmetry breaking and modes with an azimuthal $e^{im\theta}$ dependence (m an integer) appear. When the field is further intensified the free-surface disturbance becomes more complicated and eventually chaotic, drops of mercury being ejected from the surface. The growth of the $e^{im\theta}$ modes is described by a linear coupled system of equations, with periodic forcing and damping arising partly from perturbed current flow caused by the free-surface deformation and partly from nonlinear effects [7].

Many other industrial applications of MHD use alternating magnetic fields to stir a body of liquid metal or to control the shape of the free surface [1]. It has been noticed however that the field may destabilise the liquid-metal free surface, causing striations on the surface of the solidified ingot, which must be shaved off. This problem has been intensively studied [6,8,9]. Recent work [10] shows that the growth of a mode of given wavenumber is described by a simple harmonic equation forced by a convolution integral with kernel which is periodic in time. It is found that magnetic damping stabilises all modes except for

E-mail address: sneyd@math.waikato.ac.nz (A.D. Sneyd).

0997-7546/02/$ – see front matter
PII: S0997-7546(01)01171-2

certain long wavelengths with frequency close to the field frequency. We refer to this instability as the Garnier–Moreau problem after one the first papers on the subject.

All these phenomena are described by a coupled system of Mathieu–Hill equations of the form

$$\ddot{x}_i + \Omega_i^2 x_i = \varepsilon G_i(x_1, x_2, \ldots, x_N, t), \tag{1}$$

where the operators G_i are linear in the unknown functions $x_i(t)$ and periodic in time t. For the problem involving the tank of mercury with a vertical alternating field the operators G_i are *multiplicative*, i.e.

$$\boldsymbol{G}\big(\boldsymbol{x}(t)\big) = A(t)\boldsymbol{x}(t) - B(t)\dot{\boldsymbol{x}}(t),$$

where $\boldsymbol{G}$ is the $N \times 1$ vector of operators and $A(t)$, $B(t)$ are $N \times N$ periodic matrices, and $\boldsymbol{x}$ is the $N \times 1$ vector of unknown functions. In the free surface instability problem the wave spectrum is continuous and the operator takes the form of a convolution integral,

$$\boldsymbol{G}\big(\boldsymbol{x}(t)\big) = \int_{-\infty}^{\infty} K(\xi, t)\boldsymbol{x}(t-\xi)\,\mathrm{d}\xi,$$

where the $N \times N$ matrix $K(\xi, t)$ is periodic in t.

The aim of this paper is to develop simple techniques to determine the stability of the system (1), i.e. to determine whether or not there exist solutions which grow indefinitely with time. This problem (at least for multiplicative operators) has been intensively studied and detailed treatments given [11], but here we give a simple account which provides a quick path to the necessary results, based partly on the work of Russian authors [12].

The strategy is to calculate the *Floquet matrix* F which advances the solution in time by one period; if F has eigenvalues with absolute value greater than unity, the system is unstable. In Section 2 we develop a recursive method of calculating F, or more precisely a matrix which is a similarity transform of F, therefore having the same eigenvalues. Then in Section 3 we discuss in detail the case of multiplicative operators. We find that such systems exhibit similar behaviour to the simple Mathieu equation; they are generally stable (assuming positive damping) except near a *resonance* where the driving frequency is simply related to one of the natural frequencies Ω_i or to the sum or difference of two natural frequencies. Convolution operators are discussed in Section 4. Floquet theory can be applied to such systems if there exists a finite fundamental set of solutions, but it is not difficult to find examples which have infinitely many solutions. A sufficient condition is given which will guarantee the existence of a finite fundamental set for certain classes of equations. Numerical methods of solution are discussed and results given for the Garnier–Moreau problem. The free surface is stable except in the vicinity of the first resonance point. Finally Section 5 summarises our conclusions.

2. Recursion formula for the Floquet matrix

In this section we consider a system of N coupled equations. To simplify matters we take $N = 2$, but the generalisation to higher N will be clear.

We consider Eqs. (1) where i ranges from 1 to 2, and $G_i(\boldsymbol{x}, t)$ is a linear operator on

$$\boldsymbol{x} = (x_1, x_2, x_3, x_4)$$

which is periodic in t. If we make the transformation

$$z_1 = \Omega_1 x_1, \qquad z_2 = \dot{x}_1, \qquad z_3 = \Omega_2 x_2, \qquad z_4 = \dot{x}_2,$$

we can write the above set of equations as the system

$$\dot{\boldsymbol{Z}} = A\boldsymbol{Z} + \varepsilon \boldsymbol{B}(\boldsymbol{z}, t), \tag{2}$$

where A is the block matrix

$$\begin{bmatrix} \psi_1 & 0 \\ 0 & \psi_2 \end{bmatrix}, \quad \psi_i = \begin{bmatrix} 0 & \Omega_i \\ -\Omega_i & 0 \end{bmatrix},$$

and

$$\boldsymbol{B}(\boldsymbol{z}, t) = \begin{bmatrix} 0 \\ G_1(z_1/\Omega_1, z_2, z_3/\Omega_2, z_4, t) \\ 0 \\ G_2(z_1/\Omega_1, z_2, z_3/\Omega_2, z_4, t) \end{bmatrix}.$$

The Floquet matrix F for the system (1) can be written in the form

$$F = [\boldsymbol{F}_1, \boldsymbol{F}_2, \boldsymbol{F}_3, \boldsymbol{F}_4],$$

where each column vector $\boldsymbol{F}_i$ is a solution of (1), and $F(0) = I_4$ (the 4×4 identity matrix). We expand the Floquet matrix F as a power series in ε:

$$F = F_0 + \varepsilon F_1 + \varepsilon^2 F_2 + \cdots.$$

Now we can write

$$\dot{F}_n = AF_n + BF_{n-1}, \qquad F_0(0) = I_4, \qquad F_n(0) = 0 \quad (n > 0). \tag{3}$$

Here we have used the abbreviated notation,

$$BF = \big[\boldsymbol{B}(\boldsymbol{F}_1, t), \boldsymbol{B}(\boldsymbol{F}_2, t), \boldsymbol{B}(\boldsymbol{F}_3, t), \boldsymbol{B}(\boldsymbol{F}_4, t)\big].$$

Growth rates for the solutions of (2) are determined by the eigenvalues of F, but instead of working with F we use a similar matrix E [12] defined by setting

$$E = P^{-1}FP,$$

where P is the matrix which diagonalises F_0, i.e. the matrix such that

$$P^{-1}F_0P = \operatorname{diag}\big(\lambda_1^{(0)}, \lambda_2^{(0)}, \lambda_3^{(0)}, \lambda_4^{(0)}\big),$$

where

$$\lambda_i = \lambda_i^{(0)} + \varepsilon\lambda_i^{(1)} + \varepsilon^2\lambda_i^{(2)} + \cdots$$

is the ith eigenvalue of F. Now clearly,

$$F_0 = \begin{bmatrix} \cos\Omega_1 t & \sin\Omega_1 t & 0 & 0 \\ -\sin\Omega_1 t & \cos\Omega_1 t & 0 & 0 \\ 0 & 0 & \cos\Omega_2 t & \sin\Omega_2 t \\ 0 & 0 & -\sin\Omega_2 t & \cos\Omega_2 t \end{bmatrix},$$

and the matrix which carries out the diagonalisation is also block diagonal:

$$P = \begin{bmatrix} p & 0 \\ 0 & p \end{bmatrix}, \quad p = \begin{bmatrix} 1 & 1 \\ \mathrm{i} & -\mathrm{i} \end{bmatrix}, \; p^{-1} = \frac{1}{2}\begin{bmatrix} 1 & -\mathrm{i} \\ 1 & \mathrm{i} \end{bmatrix}.$$

Diagonalising F_0 gives

$$E_0 = P^{-1}F_0P = \begin{bmatrix} \mathrm{e}^{\mathrm{i}\Omega_1 t} & 0 & 0 & 0 \\ 0 & \mathrm{e}^{-\mathrm{i}\Omega_1 t} & 0 & 0 \\ 0 & 0 & \mathrm{e}^{\mathrm{i}\Omega_2 t} & 0 \\ 0 & 0 & 0 & \mathrm{e}^{-\mathrm{i}\Omega_2 t} \end{bmatrix}.$$

We can now derive a differential equation for E_n analogous to (3):

$$\dot{E}_n = P^{-1}\dot{F}_nP = P^{-1}AF_nP + P^{-1}B(F_{n-1}P, t).$$

Now since $P^{-1}F_nP = E_n$, $F_nP = PE_n$, so this last equation can be re-written:

$$\dot{E}_n = P^{-1}APE_n + P^{-1}B(PE_{n-1}, t). \tag{4}$$

A simple calculation shows that $P^{-1}AP$ is a block diagonal matrix given by

$$P^{-1}AP = \psi \text{ (say)}, = \begin{bmatrix} \psi_1 & 0 \\ 0 & \psi_2 \end{bmatrix}, \quad \psi_i = \begin{bmatrix} \mathrm{i}\Omega_i & 0 \\ 0 & -\mathrm{i}\Omega_i \end{bmatrix}.$$

Eq. (4) can now be written in the form

$$\dot{E}_n = \psi E_n + P^{-1}B(PE_{n-1}, t), \qquad E_n(0) = 0 \quad (n > 0).$$

It can be solved using the 'integrating factor' $\exp(-\psi t)$ to give

$$E_n = \exp(\psi t)\int_0^t \exp(-\psi t)P^{-1}B(PE_{n-1}, t)\,\mathrm{d}t.$$

Since our system is periodic we are particularly interested in the *period advance mapping*, namely $F(T)$ whose eigenvalues determine stability. Thus we really need to calculate

$$E_n(T) = \exp(\psi T)\int_0^T \exp(-\psi t)P^{-1}B(PE_{n-1},t)\,\mathrm{d}t. \tag{5}$$

This provides a recursive method for calculating $E_n(T)$, $n = 1, 2, \ldots$.

3. Low-frequency magnetic stirring

When a circular tank of liquid metal is stirred by a relatively weak magnetic field of frequency 1–10 Hz, axisymmetric waves are excited on the free surface [6]. As the field intensifies, non-symmetric modes proportional to $\mathrm{e}^{\mathrm{i}m\theta}$ appear, where θ is the azimuthal co-ordinate and m an integer. The free surface displacement η_m corresponding to each such mode can be written in the form

$$\eta_m = \sum_{i=1}^{\infty} x_i(t)J_m(\lambda_i r/a)\mathrm{e}^{\mathrm{i}m\theta},$$

where λ_i is the ith zero of $J'_m(x)$ and a the tank radius. The evolution equation for the $x_i(t)$ is [7]

$$\begin{aligned}&\ddot{x}_i + \frac{1}{2}\varepsilon\omega\nu_n(1-\cos\omega t)\dot{x}_i + \Omega_i^2\big[x_i + \varepsilon\sin(\omega t)u_{i\alpha}x_\alpha\big] + \varepsilon\omega\cos\omega t\, v_{i\alpha}\dot{a}_\alpha\\ &\quad= \frac{1}{8}\omega^2\varepsilon\sin(\omega t)W_{i\alpha}a_\alpha - \frac{1}{4}\omega\varepsilon(1-\cos\omega t)T_{i\alpha}\dot{x}_\alpha.\end{aligned} \tag{6}$$

Here Ω_i is the natural frequency of mode i, and $\nu_i, u_{ij}, w_{ij}, T_{ij}$ are coefficients describing nonlinear and magnetic forcing, and magnetic damping. Eq. (6) can be written in the form of (1) if we express the operator on the right-hand side as

$$G_i(\boldsymbol{x},t) = \big[a_{i\alpha}(t)\Omega_\alpha^2 x_\alpha - b_{i\alpha}(t)\Omega_\alpha\dot{x}_\alpha\big].$$

Here α is summed from 1 to infinity and

$$\begin{aligned}a_{i\alpha} &= \left[\frac{\omega^2}{8\Omega_\alpha^2}w_{i\alpha} - \frac{\Omega_i^2}{\Omega_\alpha^2}u_{i\alpha}\right]\sin\omega t,\\ b_{i\alpha} &= \frac{\omega}{4\Omega_\alpha}(\nu_i\delta_{i\alpha} + T_{i\alpha}) + \frac{\omega}{4\Omega_\alpha}(4\nu_{i\alpha} - \nu_i\delta_{i\alpha} - T_{i\alpha})\cos(\omega t).\end{aligned}$$

Parametric resonance may cause non-symmetric modes to grow and lead to further symmetry breaking; at even higher field intensities the motion becomes chaotic.

The periodic terms in this set of equations involve a single frequency ω which is twice the field frequency. In general, higher harmonics may be present so for the sake of a little more generality we assume the periodic coefficients $a_{ij}(t)$ and $b_{ij}(t)$, which can be expanded as Fourier series in the form

$$a_{ij} = a_{ij}^n\mathrm{e}^{\mathrm{i}n\omega t}, \qquad b_{ij} = b_{ij}^n\mathrm{e}^{\mathrm{i}n\omega t},$$

where we use the convention that a repeated n is summed from $-\infty$ to ∞. We suppose that the a_{ij} and b_{ij} are real, so

$$a_{ij}^{-n} = a_{ij}^{n*}, \qquad b_{ij}^{-n} = b_{ij}^{n*},$$

where the * denotes the complex conjugate. We also suppose that the (real) coefficients $b_{ii}^0 \geqslant 0$, so that the system is damped. (Indeed if this condition is not satisfied the system will always be unstable.)

The operator B is now simply represented by the block matrix

$$B = \begin{bmatrix}B_{11} & B_{12}\\ B_{21} & B_{22}\end{bmatrix}, \quad B_{ij} = \begin{bmatrix}0 & 0\\ a_{ij}\Omega_j & -b_{ij}\Omega_j\end{bmatrix}.$$

Also we find that $P^{-1}BP$ is given by

$$P^{-1}BP = C \text{ (say)}, \begin{bmatrix}C_{11} & C_{12}\\ C_{12} & C_{22}\end{bmatrix}, \quad C_{ij} = \frac{1}{2}\begin{bmatrix}\alpha_{ij}^* & -\alpha_{ij}\\ -\alpha_{ij}^* & \alpha_{ij}\end{bmatrix},$$

where $\alpha_{ij} = (-b_{ij} + \mathrm{i}a_{ij})\Omega_j$, and the asterisk denotes a complex conjugate. The recursion formula (5) for E_n now assumes the form

$$E_n = \exp(\psi t) \int_0^t \exp(-\psi t) C E_{n-1}\, \mathrm{d}t. \tag{7}$$

In magnetic stirring the interaction parameter ε will be small, so the relatively simple calculation of E_1 is sufficiently accurate. When we apply (7) to

$$E_0 = \begin{bmatrix} \exp(\psi_1 t) & 0 \\ 0 & \exp(\psi_2 t) \end{bmatrix},$$

the integrand of (7) assumes the form

$$\begin{bmatrix} \exp(-\psi_1 t) & 0 \\ 0 & \exp(-\psi_2 t) \end{bmatrix} \begin{bmatrix} C_{11} & C_{12} \\ C_{21} & C_{22} \end{bmatrix} \begin{bmatrix} \exp(\psi_1 t) & 0 \\ 0 & \exp(\psi_2 t) \end{bmatrix} = \begin{bmatrix} D_{11} & D_{12} \\ D_{21} & D_{22} \end{bmatrix}.$$

Here,

$$D_{ij} = \exp(-\psi_i t) C_{ij} \exp(\psi_j t) = \frac{1}{2} \begin{bmatrix} \beta^*_{Dij} & -\beta^*_{Sij} \\ -\beta_{Sij} & \beta_{Dij} \end{bmatrix} \tag{8}$$

and

$$\beta_{Dij} = \alpha_{ij} \mathrm{e}^{\mathrm{i}t(\Omega_i - \Omega_j)}, \qquad \beta_{Sij} = \alpha^*_{ij} \mathrm{e}^{\mathrm{i}t(\Omega_i + \Omega_j)}. \tag{9}$$

The general formula for E_1 is therefore

$$E_1(T) = \exp(\psi T) \int_0^T \begin{bmatrix} D_{11} & D_{12} \\ D_{21} & D_{22} \end{bmatrix} \mathrm{d}t. \tag{10}$$

3.1. Non-resonance

We begin by assuming that all the eigenvalues (or diagonal elements) are different, i.e. that

$$E^{\pm \mathrm{i}\Omega_i T} \neq \mathrm{e}^{\pm \mathrm{i}\Omega_j T} \quad \text{for any } (i, j).$$

To first order in ε Theorem 1 of Appendix A shows that we need calculate only the diagonal elements of $E_1(T)$. Using (8), (9) and (10) we find that the first element of $E_1(T)$ is given by

$$(D_{11})_{11} = -\frac{1}{2} \varepsilon T \mathrm{e}^{\mathrm{i}\Omega_1 T} (b_{11} + \mathrm{i}a_{11}),$$

and to $\mathrm{O}(\varepsilon)$ the first eigenvalue is given by

$$\lambda = \mathrm{e}^{\mathrm{i}\Omega_1 T} \left[1 - \frac{1}{2} \varepsilon \Omega_1 T \mathrm{e}^{\mathrm{i}\Omega_1 T} \left(b^0_{11} + \mathrm{i}a^0_{11} \right) \right] = \lambda^{(0)}_1 + \varepsilon \lambda^{(1)}_1.$$

Since we have assumed $b^0_{11} \geqslant 0$ the system is stable (marginally stable if $b_{11} = 0$). Other eigenvalues are given by similar formulae.

3.2. Resonances

When two eigenvalues of E_0 are equal, Theorem 3 of Appendix A shows that a different scheme for calculating the $\mathrm{O}(\varepsilon)$ eigenvalue perturbations must be used. There are three possible ways for eigenvalues to coincide – firstly we may find

$$\mathrm{e}^{\mathrm{i}\Omega_i T} = \mathrm{e}^{-\mathrm{i}\Omega_i T}, \quad \Omega_i = \frac{1}{2} m\omega, \ m = 1, 2, \ldots,$$

in which case we say we have a type I resonance. A type II resonance occurs when

$$\mathrm{e}^{\mathrm{i}\Omega_i T} = \mathrm{e}^{-\mathrm{i}\Omega_j T}, \quad \Omega_i + \Omega_j = m\omega.$$

In this case two pairs of eigenvalues are equal since $\lambda^{(0)}_i = \lambda^{(0*)}_j$ and $\lambda^{(0*)}_i = \lambda^{(0)}_j$. Finally we may have a type III resonance, with

$$\mathrm{e}^{\mathrm{i}\Omega_i T} = \mathrm{e}^{\mathrm{i}\Omega_j T}, \quad \Omega_i - \Omega_j = m\omega,$$

again giving two pairs of equal eigenvalues.

3.3. Type I resonance

First we analyse stability in the vicinity of the type I resonance at frequency

$$2\Omega_1/m = \omega_0 \text{ say}, \quad \text{so that} \quad e^{i\Omega_1 T} = e^{-i\Omega_1 T} = e^{i\pi m},$$

where m is a positive integer. Taking ω close to the resonant frequency we write

$$\omega = \omega_0(1+\varepsilon\nu), \qquad T = T_0(1-\varepsilon\nu), \tag{11}$$

where $T_0 = 2\pi/\omega_0$ is the period at the exact resonance point. Now Theorem 3 and (10) show that we need to consider the matrix

$$\begin{pmatrix} e^{i\Omega_1 T} & 0 \\ 0 & e^{-i\Omega_1 T} \end{pmatrix} \left(I_2 + \varepsilon \int_0^T D_{11}\,dt \right),$$

which can be expanded to $O(\varepsilon)$ in the form

$$e^{i\pi m}\left[\begin{pmatrix} 1 & 0 \\ 0 & 1 \end{pmatrix} + \varepsilon i\pi m\nu \begin{pmatrix} -1 & 0 \\ 0 & 1 \end{pmatrix} + \varepsilon \int_0^{T_0} D_{11}\,dt \right]. \tag{12}$$

We use (10) to evaluate the matrix D_{11}. If we write an eigenvalue λ of the matrix (12) in the form

$$\lambda = e^{i\pi m}(1+\varepsilon\lambda_1)$$

then Theorem 3 shows that λ_1 is an eigenvalue of the matrix

$$\frac{1}{2}\pi m \begin{pmatrix} -2i\nu - c_0 & c_m^* \\ c_m & 2i\nu - c_0^* \end{pmatrix},$$

where $c_m = b_{11}^m + ia_{11}^m$. The eigenvalues are easily found:

$$\frac{2\lambda_1}{m\pi} = -b_{11}^0 \pm \left[|c_m|^2 - \left(a_{11}^0 + 2\nu\right)^2\right]^{1/2}.$$

A positive value of λ_1 – and hence an instability – will occur only if

$$|c_m| > |b_{11}^0|,$$

i.e. only if the damping is not too strong. The growth rate will then be $\varepsilon\lambda_1/T_0$. Marginal stability occurs when $\lambda_1 = 0$ or

$$\nu = \frac{1}{2\pi}\left[-a_{11}^0 \pm \left[|c_m|^2 - \left(b_{11}^0\right)^2\right]^{1/2}\right] = \nu_1,\ \nu_2 \text{ say}. \tag{13}$$

From the definition of ν in (11) it follows that

$$\varepsilon = \frac{\omega - \omega_0}{\nu\omega_0},$$

so the the stability boundaries in the (ω, ε)-plane are straight lines emanating from the resonance point $(\omega_0, 0)$ with slopes $1/(\omega_0\nu_i)$, $i = 1, 2$. Note that as $b_{11}^0 \to |c_m|^2$ from below the wedge-shaped region of instability narrows and eventually disappears. This is because the damping parameter b_{11}^0 is proportional to ε. The case of a fixed damping constant is considered in Section 3.6.

To investigate the accuracy of the first-order theory, we compare exact and approximate stability boundaries of the equation

$$\ddot{x} + x = \varepsilon\left[a\sin(\omega t)x - \left(b + c\cos(\omega t)\right)\dot{x}\right],$$

where a, b and c are constants. Results are shown in Fig. 1 for the $\omega = 2$ resonance. The exact numerical calculation was performed by using the NAG subroutines D02BJF to calculate the Floquet matrix, and F02EBF to find its eigenvalues. The stability boundary was then tracked using a form of bisection method.

We set $a = 1$, $c = 0.5$, and choose different b values to illustrate the narrowing of the stability boundaries. The exact boundaries are tangential to the approximate wedge at the resonance point $2, 0$ but diverge for larger values of ε. For $\varepsilon < 0.1$ the accuracy is reasonable.

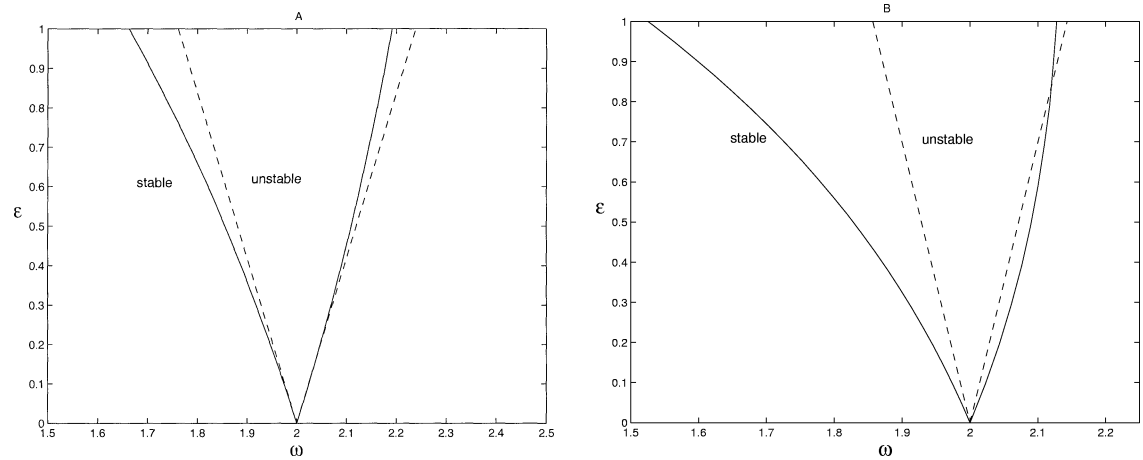

Fig. 1. Exact and approximate stability boundaries. In A, $b = 0$ and in B, $b = 0.6$. The continuous curves represent the exact stability boundaries, and the dashed curves the approximate instability wedge.

3.4. Type II resonance

Suppose for example that $e^{i\Omega_1 T} = e^{-i\Omega_2 T}$ and the resonant frequency

$$\omega_0 = (\Omega_1 + \Omega_2)/m \quad (m \text{ an integer}).$$

We analyse stability in the vicinity of this resonance point, writing $\omega = \omega_0(1 + \varepsilon\nu)$, so that

$$e^{i\Omega_i T} = e^{ip_i}(1 - i\varepsilon p_i \nu), \quad p_i = 2\pi\Omega_i/\omega_0. \tag{14}$$

Following Theorem 3 of Appendix A with $p = 1$ and $q = 4$ we consider the $O(\varepsilon)$ terms of the matrix

$$\begin{pmatrix} (E)_{11} & (E)_{14} \\ (E)_{41} & (E)_{44} \end{pmatrix}.$$

Using (14) and (10) we can show that the eigenvalues are of the form

$$\lambda = e^{ip_1}(1 + \varepsilon\lambda_1),$$

where λ_1 is an eigenvalue of the matrix

$$\frac{1}{2}\begin{pmatrix} -2ip_1\nu - p_1 c_{011} & -p_2 d^*_{m12} \\ p_1 d^*_{m21} & 2ip_2\nu - p_2 c^*_{022} \end{pmatrix}. \tag{15}$$

Here

$$c_{mij} = b^m_{ij} + ia^m_{ij}, \qquad d_{mij} = b^m_{ij} - ia^m_{ij}.$$

It is difficult to write down a general criterion for instability, but as an illustration we consider two coupled equations:

$$\ddot{x}_i + 2\varepsilon k_i \Omega_i(1 + \cos\omega t)\dot{x}_i + \Omega_i^2 x_i = \varepsilon\Omega_i^2 \sin\omega t a_{i\alpha} x_\alpha, \quad i = 1,\ 2. \tag{16}$$

The matrix (15) then takes the form

$$\begin{pmatrix} -ip_1\nu - p_1 k_1 & -\frac{1}{4}p_2 a_{12} \\ -\frac{1}{4}p_1 a_{21} & ip_2\nu - p_2 k_2 \end{pmatrix}.$$

Solving the quadratic eigenvalue equation for λ_1 shows that the system is unstable near this resonance point only if

$$a_{12}a_{21} > 16k_1k_2$$

and that the instability region lies between the pair of straight lines,

$$\frac{\omega - \omega_0}{\omega_0} = \pm\frac{\varepsilon k_s}{2\pi}\left[\frac{a_{12}a_{21}}{16k_1k_2} - 1\right]^{1/2}, \tag{17}$$

where $k_s = p_1k_1 + p_2k_2$.

3.5. Type III resonance

In this case $e^{i\Omega_1 T} = e^{i\Omega_2 T}$ and

$$\omega = \frac{\Omega_1 - \Omega_2}{m} = \omega_0 \text{ say}, \quad m \text{ an integer.}$$

To analyse stability in the vicinity of the resonance point we write $\omega = \omega_0(1 + \varepsilon\nu)$, and the analysis and notation follow closely those of the previous subsection. Following Theorem 3 of Appendix A with $p = 1$ and $q = 3$ we consider the $O(\varepsilon)$ terms of the sub-matrix

$$\begin{pmatrix} (E)_{11} & (E)_{13} \\ (E)_{31} & (E)_{33} \end{pmatrix}.$$

Using (14) and (10) we can show that the eigenvalues are of the form

$$\lambda = e^{ip_1}(1 + \varepsilon\lambda_1),$$

where λ_1 is an eigenvalue of the matrix

$$\frac{1}{2}\begin{pmatrix} -2ip_1\nu - p_1 c_{011} & -p_2 c^*_{m12} \\ -p_1 d^*_{m21} & 2ip_2\nu - p_2 d_{022} \end{pmatrix}.$$

Again we examine the particular system (16); the quadratic equation for $\lambda_1^{(1)}$ shows that instability occurs only if

$$a_{12}a_{21} < -16k_1k_2.$$

The instability region is bounded by the pair of straight lines

$$\frac{\omega - \omega_0}{\omega_0} = \pm\frac{\varepsilon k_s}{2\pi}\left[\frac{|a_{12}a_{21}|}{16k_1k_2} - 1\right]^{1/2}. \tag{18}$$

Fig. 2 compares exact numerically-calculated stability boundaries for (16) with those predicted by the asymptotic formulae (17) and (18). In Fig. 2A we have chosen $\Omega_1 = 1$ and $\Omega_2 = 2$, so that there are type I resonances at $\omega = 2$ and $\omega = 4$, and a type II resonance at $\omega = 3$. We also took $k_1 = k_2 = 0.05$ and the matrix of coefficients

$$\begin{pmatrix} a_{11} & a_{12} \\ a_{21} & a_{22} \end{pmatrix} = \begin{pmatrix} 1.0 & 0.3 \\ 0.5 & 1.0 \end{pmatrix}.$$

With this coefficient matrix the potential type III resonance at $\omega = 1$ does not in fact occur. In Fig. 2B the sign of a_{21} in the coefficient matrix was changed, so that now we see only a type III resonance. (The complicated shape of the left-most stability boundary is probably due to an accumulation of weak higher-order resonances near $\omega = 0$.)

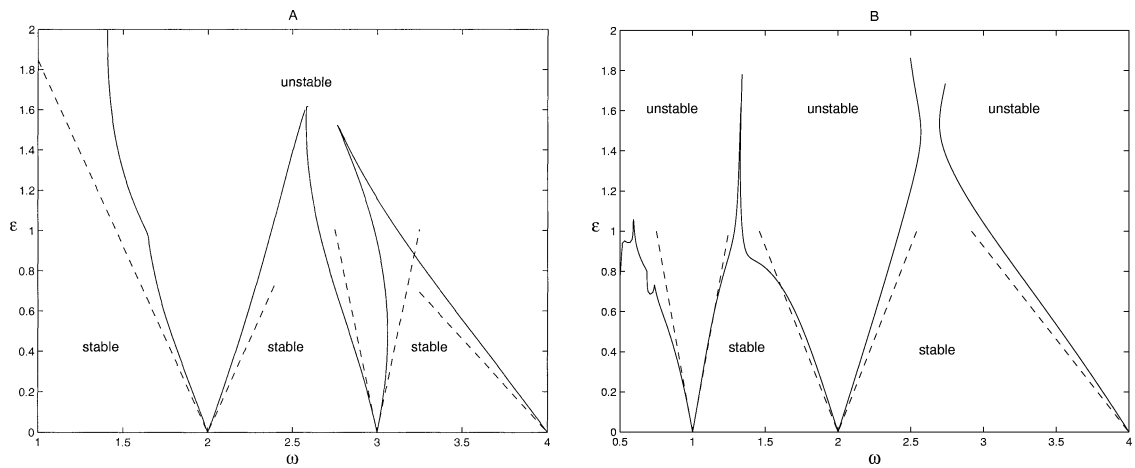

Fig. 2. Exact and approximate stability boundaries. A shows a type II resonance, and B a type III resonance. The continuous curve is the exact boundary and the dashed lines the approximations (17) and (18).

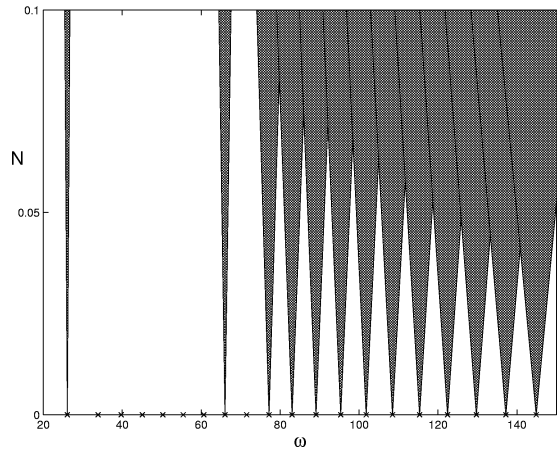

Fig. 3. Instability regions (shaded) for the $m = 5$ type I modes in magnetic stirring. The crosses on the ω-axis mark the resonance points.

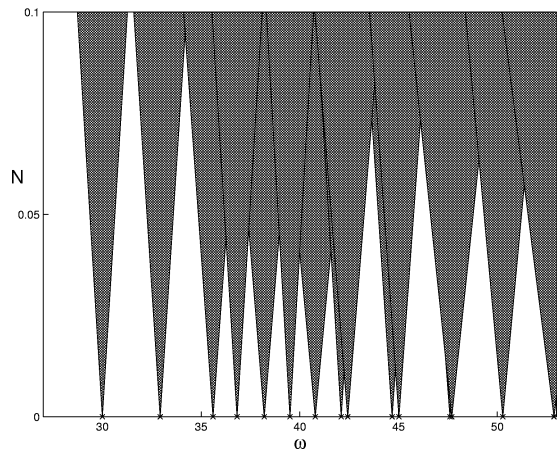

Fig. 4. Instability regions (shaded) for the $m = 5$ type II modes in magnetic stirring. The crosses on the ω-axis mark the resonance points.

3.6. Magnetic stirring results

Fig. 3 shows instability regions for type I resonance of the $m = 5$ mode. (For different m the picture is very similar.) A consequence of electromagnetic damping is that not all resonance points trigger an instability. The lowest natural frequency Ω_1 always gives rise to an instability region; Ω_2 to Ω_7 and Ω_9 do not. But then Ω_8, Ω_{10} and all subsequent natural frequencies have associated regions of instability, which widen as Ω_n increases.

Fig. 4 shows instability regions for $m = 5$ type II resonances. Here it appears that every resonance point gives rise to an instability region. In this application however, no type III resonance appears to be destabilising. The combined type I and type II instability regions are shown in Fig. 5.

4. Convolution operators

4.1. General considerations

In this section we analyse equations of the form (1) where the operator G is given by

$$G_i(x,t) = \int_{-\infty}^{\infty} K_\alpha(\xi,t)x_\alpha(t-\xi)\,\mathrm{d}\xi, \tag{19}$$

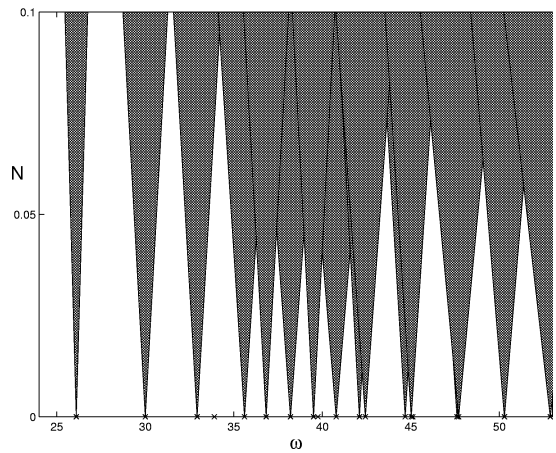

Fig. 5. Instability regions (shaded) for the $m = 5$ type I and II modes in magnetic stirring. The crosses on the ω-axis mark the resonance points.

and the kernel functions $K_\alpha(\xi, t)$ are periodic in t with period T. Note that the form (19) includes operators such as

$$\int_{-\infty}^{\infty} K(\xi, t)\dot{x}(t-\xi)\,\mathrm{d}\xi = \int_{-\infty}^{\infty} K_\xi(\xi, t)x(t-\xi)\,\mathrm{d}\xi$$

assuming that $K \to 0$ as $\xi \to \pm\infty$.

Such a system arises for example when studying the Faraday experiment with viscous damping [5]. The equations take the form

$$\ddot{a}_n + \Omega_n^2\big[1 + \varepsilon\sin(\omega t)\big]a_n = \varepsilon \int_{-\infty}^{\infty} F(\xi)A_{n\alpha}\dot{a_\alpha}(t-\xi)\,\mathrm{d}\xi,$$

where the $a_n(t)$ are coefficients in a Fourier series representation of the free surface, the Ω_n are natural oscillation frequencies, and the $A_{n\alpha}$ are viscous damping constants. Here the kernel is a function of ξ only and the system can be analysed simply by taking a Fourier transform. Viscosity rounds off the tips of the typical wedges associated with the undamped Mathieu equation, and the instability region separates from the ω axis and shifts towards the origin. A curious result is that the point P for example in the (ω, ε)-plane which was stable in absence of viscosity, is destabilised by the presence of viscosity (Fig. 6).

A single equation of similar form but with a time-dependent Kernel describes the stability of a liquid metal free surface in the presence of a horizontal alternating magnetic field [10]. We shall our discussion of this more difficult problem to the case of a single equation.

In these examples the convolution operator arises because a Fourier transform is used to solve a certain sub-problem. In the Faraday experiment with viscosity, flow in the time-dependent boundary-layer on the base and walls of the tank must be solved using a Fourier transform. In the Garnier–Moreau problem Fourier analysis is necessary to solve for the diffusion of magnetic field into the liquid metal. Inversion of the Fourier transform then leads to a convolution integral. An unusual feature of such problems is that the equation involves values of the unknown function $x(t)$ say at all times. Solving the magnetic field diffusion problem for example at $t = t_0$ requires knowledge of the surface magnetic field for all $t < t_0$, or alternatively the complete field distribution $B(z, 0)$ at some initial instant $t = 0$. To analyse stability we monitor the growth of a very small disturbance

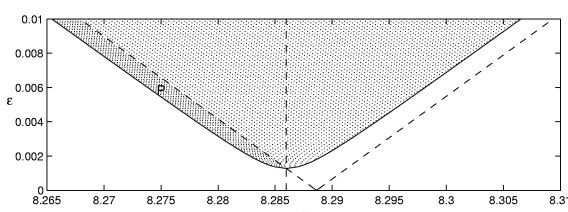

Fig. 6. Instability regions for the Faraday experiment. The sloping dashed straight lines represent the stability boundary with zero viscosity, and the continuous curved line, the boundary when viscosity is included.

beginning in the distant past, so there is no 'initial instant', and a Fourier transform (rather than a Laplace transform) is the natural method of analysis.

It seems plausible that the equation

$$\ddot{x} + \Omega^2 x = \varepsilon \int_{-\infty}^{\infty} K(\xi, t) x(t-\xi)\,\mathrm{d}\xi, \tag{20}$$

with initial conditions $x(0) = a, \dot{x}(0) = b$ will have a unique solution for ε sufficiently small. For if we expand x in the form

$$x = x_0 + \varepsilon x_1 + \varepsilon^2 x_2 + \cdots$$

then the initial-value problem for x_0,

$$\ddot{x}_0 + \Omega^2 x_0 = 0; \qquad x_0(0) = a, \qquad \dot{x}_0(0) = b,$$

has a unique solution, and the x_n for $n \geqslant 1$ are determined recursively by solving the well-posed initial-value problems

$$\ddot{x}_n + \Omega^2 x_n = \int_{-\infty}^{\infty} K(\xi, t) x_{n-1}(t-\xi)\,\mathrm{d}\xi; \qquad x_n(0) = 0, \qquad \dot{x}_n(0) = 0.$$

However further solutions may exist if the Fourier transform of K has singularities. Consider the special case in which K is independent of t, for which a complete analysis is possible. Taking the Fourier transform in time of (20) we find

$$\left[\Omega^2 - \alpha^2 - \varepsilon \widehat{K}(\alpha)\right]\hat{x} = 0 \quad \text{or} \quad H(\alpha)\hat{x} = 0 \quad \text{say}, \tag{21}$$

where the hat indicates the transformed function. This equation has solutions of the form

$$\hat{x} = \delta(\alpha - \alpha_i), \qquad x = \mathrm{e}^{-\mathrm{i}\alpha_i t},$$

where α_i is a zero of $H(\alpha)$. Thus the number of independent solutions is equal to the number zeros of H. If $\widehat{K}$ is meromorphic and $\mathrm{o}(\alpha^2)$ at infinity then a well known theorem of complex analysis [13] shows that

$$N - P = 2,$$

where N is the number of zeros of H and P the number of poles. Thus $N = P + 2$, and if H has poles there will exist more than 2 independent solutions. For example take $K(\xi) = \mathrm{e}^{-|\xi|}$ then $\widehat{K}(\alpha) = 2/(1+\alpha^2)$, and we find $N = 4$. The equation

$$\ddot{x} + \Omega^2 x = \varepsilon \int_{-\infty}^{\infty} \mathrm{e}^{-|\xi|} x(t-\xi)\,\mathrm{d}\xi \tag{22}$$

therefore has *four* independent solutions $\mathrm{e}^{-\mathrm{i}\alpha_i t}$, $i = 1{-}4$. For small ε the α_i are given by

$$\alpha = \pm\left(\Omega - \frac{2\varepsilon}{\Omega(1+\Omega^2)}\right), \qquad \alpha = \pm\mathrm{i}\left(1 - \frac{2\varepsilon}{1+\Omega^2}\right).$$

Two of the zeros are perturbations of $\alpha = \pm\Omega$, and the other two lie near the poles $\alpha = \pm i$.

For some kernel functions (20) may have infinitely many independent solutions. For example let $K(\xi, t) = \mathrm{e}^{-\xi^2}$; then taking the Fourier transform of (20) we obtain (21) with

$$H(\alpha) = \Omega^2 - \alpha^2 - \varepsilon\sqrt{\pi}\,\mathrm{e}^{-\alpha^2/4}.$$

It is shown in the appendix that H has *infinitely many* zeros and consequently (20) has infinitely many independent solutions.

Our main concern is discover the conditions under which (20) will possess a *fundamental set of solutions*, i.e. a finite basis for the vector space of solutions. Certainly (22) has a fundamental set, even though it is twice as large as we might have expected! Our last example however does not. In the rest of this subsection we establish sufficient more general conditions under which the existence of a fundamental set can be guaranteed.

Suppose that the kernel function can be expanded as a finite Fourier series in the form

$$K(\xi, t) = \sum_{n=-N}^{N} a_n(\xi)\mathrm{e}^{\mathrm{i}n\omega t}.$$

Then taking the Fourier transform of (20) with respect to t we obtain

$$\left(\Omega^2 - \alpha^2\right)\hat{x} = \varepsilon \sum_{n=-N}^{N} \hat{a}_n(\alpha + n\omega)\hat{x}(\alpha + nw). \tag{23}$$

Now suppose that each $\hat{a}$ is a meromorphic with a finite number of poles P_n say, and can be expanded in the form

$$\hat{a}_n(\alpha) = \sum_{m=1}^{P_n} \frac{b_{nm}}{\alpha - \alpha_{nm}},$$

where b_{nm} and α_{nm} are constants. Then multiplying (23) by the common denominator of the $\hat{a}_n$ we obtain an equation of the form

$$p(\alpha)\hat{x} = \varepsilon \sum_{n=-N}^{N} p_n(\alpha)\hat{x}(\alpha + n\omega),$$

where $p(\alpha)$ and the $p_n(\alpha)$ are polynomials. Fourier inversion gives

$$D(x) = \varepsilon \sum_{n=-N}^{N} D_n\left(\mathrm{e}^{\mathrm{i}n\omega t}x\right),$$

where D and the D_n are differential operators with respect to t. This is a linear differential equation and will therefore have a fundamental set of solutions. The number of independent solutions is the order of the differential operator D, which is equal to the order of the polynomial p.

In many applications the most important question is whether or not solutions of (20) are stable, and in the following sections we consider approximate and exact methods of stability analysis.

4.2. Stability analysis by time-averaging

If the frequency ω of the kernel function K is much greater that the natural oscillation frequency Ω, we can take a time-average of (20) over one period $T = 2\pi/\omega$. Over such a short time-interval x is regarded as constant, and we obtain

$$\ddot{x} + \Omega^2 x = \varepsilon \int_{-\infty}^{\infty} \overline{K}(\xi)x(t-\xi)\,\mathrm{d}\xi, \quad \overline{K}(\xi) = T^{-1}\int_0^T K(\xi, t)\,\mathrm{d}t. \tag{24}$$

This approximation has been used by a number of authors to study instability of a liquid-metal free surface in the presence of a high-frequency alternating magnetic field [14,9]. Taking the Fourier transform in time of (24) we obtain

$$H(\alpha)\hat{x} = 0, \quad H(\alpha) = \Omega^2 - \alpha^2 - \varepsilon\widehat{\overline{K}}, \tag{25}$$

and the solutions are $x = \mathrm{e}^{-\mathrm{i}\alpha_i t}$ where the α_i are the zeros of H. The system is unstable if there exists a zero of H with negative imaginary part. Using the notation of Fautrelle and Sneyd [15] the averaged kernel function for alternating field problem is given by

$$\widehat{\overline{K}}(\alpha) = \frac{k(1-\mathrm{i})}{\kappa + \chi(\alpha+\omega)} + \frac{k(1+\mathrm{i})}{\kappa^* + \chi(\alpha-\omega)},$$

where

$$\kappa = k + (1+\mathrm{i})/\delta, \qquad \chi(\alpha) = \left(k^2 - \mathrm{i}\alpha/\lambda\right)^{1/2}.$$

Here k is the wavenumber of the surface wave, δ the magnetic skin depth, and λ the magnetic diffusivity of the liquid metal. The branch of square root is chosen to give χ a positive real part. In order to ensure that H is analytic two cuts must be made in the complex plane; these are parallel to the imaginary axis, extending from the points $\alpha = -\mathrm{i}k^2\lambda \pm \omega$ to $-\mathrm{i}\infty$. Rouché's theorem [13] then shows that H has just two zeros, which for small ε are perturbations of $\pm\Omega$. These are readily calculated numerically, and a weak instability is found.

4.3. Floquet matrix method

Stability may be determined by calculating the Floquet matrix to leading order, as discussed in Section 2. Using the methods of that section we find that

$$E_0 + \varepsilon E_1 = \begin{pmatrix} e^{i\Omega T}\left[1 + \frac{\varepsilon T \widehat{\overline{K}}(-\Omega)}{2i\Omega}\right] & O(\varepsilon) \\ O(\varepsilon) & e^{-i\Omega T}\left[1 - \frac{\varepsilon T \widehat{\overline{K}}(\Omega)}{2i\Omega}\right] \end{pmatrix}.$$

Instability occurs if either of the eigenvalues of this matrix has absolute value greater than 1, i.e. if

$$\Im\{\widehat{\overline{K}}(-\Omega)\} > 0 \quad \text{or} \quad \Im\{\widehat{\overline{K}}(\Omega)\} < 0. \tag{26}$$

Curiously this result is the same to $O(\varepsilon)$ as that found by time-averaging. If we calculate the zeros of $H(\alpha)$ (see (25)) to $O(\varepsilon)$, we find

$$\alpha = \Omega - \frac{\varepsilon}{2\Omega}\widehat{\overline{K}}(\Omega), \qquad \alpha = -\Omega + \frac{\varepsilon}{2\Omega}\widehat{\overline{K}}(-\Omega).$$

The system is unstable if either of these expressions has a positive imaginary part, which is equivalent to condition (26), and the corresponding expressions for the growth rates are also equal. It is surprising that these two quite different approximations – one based on large ω and the other on small ε yield the same instability criteria.

4.4. Numerical methods

Suppose the kernel function can be expanded as a finite Fourier series:

$$K(\xi, t) = \sum_{m=-M}^{M} a_m(\xi) e^{im\omega t}, \tag{27}$$

and that a fundamental set of solutions exists. Then according to the well-known result of Floquet theory [16], the fundamental solutions can be written in the form

$$e^{ist} \sum_{n=-\infty}^{\infty} \alpha_n e^{in\omega t}, \tag{28}$$

where s is a constant which determines the growth rate or decay rate of the solution. The system will be unstable if the imaginary part of s is negative for any fundamental solution. We note that there is some redundancy involved in the representation (28) – if we make the transformation $s \to s + p\omega$, $\alpha_n \to \alpha_{n+p}$, where p is an integer, the fundamental solution (28) is unchanged. Without loss of generality we can assume the $-\omega/2 \leqslant \Re(s) \leqslant \omega/2$.

Substituting this solution form into (20), and equating coefficients of $e^{in\omega t}$ we obtain a system of equations

$$(\Omega^2 - s_n^2)\alpha_n = \varepsilon \sum_{m=-M}^{M} \alpha_{m-n}\hat{a}_n(-s_{m-n}), \quad n = 0, \pm 1, \pm 2, \ldots,$$

where $s_n = s + n\omega$.

If we truncate the series (28) to $2N + 1$ terms say (summing from $n = -N$ to N), the above system can be written in the form

$$A(s)\boldsymbol{\alpha} = 0, \quad \boldsymbol{\alpha}^{\mathrm{T}} = (\alpha_{-N}, \ldots, \alpha_{-1}, \alpha_0, \alpha_1, \ldots, \alpha_N).$$

The matrix $A(s)$ has an $2M + 1$-diagonal structure, i.e. in each row there are M non-zero elements on either side of the leading diagonal, the growth rate s can be found by solving

$$\det A(s) = F(s)\,(\text{say}) = 0. \tag{29}$$

In principle (29) can be solved numerically – for example by the Newton–Raphson method – to determine the zero with maximum negative imaginary part, but this method is fraught with difficulties. When a derivative is required, each iteration involves computing $2N + 2(2N + 1) \times (2N + 1)$ determinants (1 for $A(s)$ and $2N + 1$ for $A'(s)$). Care must be taken to ensure that *all* zeros are found, since different initial guesses may converge to the same value. Nevertheless the method may be feasible provided M is small, and not too large a value of N is necessary for convergence. For example in the alternating field problem [10] the matrix A is tridiagonal ($M = 1$), which means only a simple computation is necessary to evaluate the determinants, and it was found in practice that a Fourier series truncation of $N = 3$ gives accurate results. To ensure that all

zeros were found, the calculation was first performed for parameter values which yielded simple estimates of the zeros; then the parameter values we gradually changed, the results of the previous calculation being used as initial estimates for the next.

An alternative method for estimating the largest negative real part of the zeros of $F(s)$ is based on the well-known result,

$$\Delta_{\mathcal{C}}\mathrm{Arg}\, f(z) = 2\pi(N_0 - P)$$

for the change in argument of an analytic function around a closed contour $\mathcal{C}$. Here N_0 is the number of zeros and P the number of poles of $f(z)$ inside $\mathcal{C}$. The chosen contour consists of the straight line segment $\Im(s) = b$ completed by a semi-circle in the lower half of the complex plane (Fig. 7). We take AB so long that the semi-circle can include all zeros in the lower half-plane.

Assuming that $\hat{a}_n(s) = o(s^2)$ then $F(s) \approx s^{4N+2}$ as $|s| \to \infty$, and the change in argument of $F(s)$ around the semi-circle is $(2N+1)\pi$. The number $n(b)$ of zeros of $F(s)$ lying below AB is therefore given by

$$n_b = 2N + 1 - \Delta_{AB}\mathrm{Arg}\big(F(s)\big).$$

The change in argument in $F(s)$ is readily calculated by stepping along AB. If this line passes close to a zero the argument may change rapidly so it was found necessary control the step length to prevent any increment in the argument exceeding 0.2 radians. A bisection method was then used to locate the value of b, say b_c at which n_b becomes zero; b_c then equals the largest negative imaginary part of any zero, and hence the growth rate of the instability. This method proved to be very robust.

A typical set of results for the alternating field problem [10] is shown in Fig. 8 as graphs of growth rate versus the wavenumber k of the surface wave.

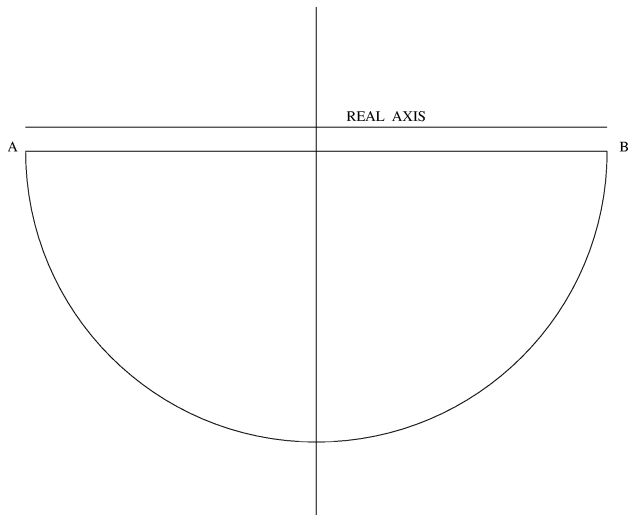

Fig. 7. Contour $\mathcal{C}$ in the complex plane.

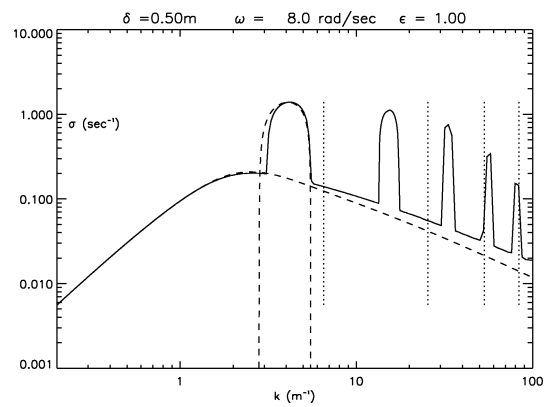

Fig. 8. Graph of growth rate versus wavenumber k.

4.5. Resonance

The most remarkable feature of the results is a series of sharp peaks in the growth rate, which occur near *resonance* points where the gravity-capillary frequency Ω is an integral multiple of the applied frequency ω:

$$\Omega = m\omega, \quad m = 1, 2, 3, \ldots.$$

(The positions of the resonances are marked by vertical dotted lines.) In order to understand these peaks we assume that ε is small. To leading order in ε the matrix A is diagonal, and the zeros are given by

$$s = -2n\omega \pm \Omega, \quad -N \leqslant n \leqslant N.$$

Two zeros corresponding to $n = n_1$, $n = n_2$ are equal if

$$\Omega = (n_1 - n_2)\omega,$$

i.e. if we are at a resonance point. It appears therefore that the imaginary part of nearly coincident zeros grows very rapidly in the vicinity of a resonance point, but is relatively small everywhere else.

To demonstrate this we truncate the system of equations to $N = 1$ so that we are dealing with a 3×3 matrix A. The diagonal elements written to leading order and in dimensionless form are:

$$(1 + s' - 2w)(1 - s' + 2w), \qquad (1 + s')(1 - s'), \qquad (1 + s' + 2w)(1 - s' - 2w),$$

where $s' = s/\Omega$ and $w = \omega/\Omega$. At the first resonance $w = 1$ the zeros $s' = \pm 1$ are repeated, and we consider in detail the behaviour of the former zero in this neighbourhood, writing

$$s' = 1 + \varepsilon\delta_s, \qquad w = 1 + \varepsilon\delta_w.$$

The equation $\det(A) = 0$ can now be written to first order in ε in the form

$$\begin{vmatrix} 2\varepsilon(\delta_s - 2\delta_w) + \varepsilon\hat{a}_0(\Omega) & \varepsilon\hat{a}_{-1}(\Omega) & \varepsilon\hat{a}_{-2}(\Omega) \\ \varepsilon\hat{a}_1(-\Omega) & -2\varepsilon\delta_s + \varepsilon\hat{a}_0(-\Omega) & \varepsilon\hat{a}_{-1}(-\Omega) \\ \hat{a}_2(-3\Omega) & \varepsilon\hat{a}_1(-3\Omega) & -8 \end{vmatrix} = 0.$$

Dividing the first two rows of the determinant by ε and then letting $\varepsilon \to 0$ we find that δ_s satisfies a quadratic with solution

$$\delta_s = \delta_w - \frac{1}{2}\mathrm{i}\hat{a}_{0I} \pm \frac{1}{2}\left[(2\delta_w - \hat{a}_{0R})^2 - |\hat{a}_{-1}|^2\right]^{1/2}, \tag{30}$$

where the $\hat{a}_i$ coefficients are all evaluated at Ω and the subscripts R, I indicate real and imaginary parts. The corresponding growth rate $-\varepsilon\Im(\delta_s)$ is also shown as a dashed curve in Fig. 8. Clearly, the growth rate corresponding to this zero is usually negative, but increases rapidly near a resonance point, outstripping the growth rates yielded by the other zeros. Eq. (30) shows that maximum growth rate occurs at $\delta_w = -\hat{a}_{0R}/2$ – a point lying slightly to the left of the resonance point. As ε becomes smaller, the resonance point and point of maximum growth rate tend to coincide more closely, as expected. The maximum growth rate can also be predicted from (30) to be $(|\hat{a}_1|^2 - \hat{a}_{0I})/2$. This is much larger than typical values away from the resonance point, since the real parts of the $\hat{a}_i$ coefficients are generally much larger than the imaginary parts in this particular application.

It is easily verified that the other repeated zero $s' = -1$ gives an identical growth rate. The behaviour at other resonance points can be described by quadratic equations using similar methods, but the algebra becomes more complicated, since to deal with the resonance $\Omega = n\omega$ one needs to consider a $(2n + 1) \times (2n + 1)$ determinant.

5. Conclusions

Floquet theory can be used to analyse the stability of equations of the form (1) when the operators are multiplicative. A first-order perturbation in the small amplitude parameter ε provides a complete classification except in degenerate cases when a formula such at (13) predicts neutral stability because $c_0 = c_m = 0$. Then an expansion up to $\mathrm{O}(\varepsilon^2)$ is necessary to determine stability; the recursion formula (5) is applied twice, and the algebra becomes more complicated. Comparison of first-order approximations with exact numerical results for system of equations with coefficients of order unity, shows that our formulae are quite accurate if $\varepsilon < 0.1$.

Convolution operators are more difficult because the system may not have a finite fundamental set of solutions. We have established a sufficient condition for the existence of a fundamental set, but more work is necessary for a complete analysis. Trial solutions of the form (28) however can provide a lower-bound for growth rates, even when Floquet analysis is not strictly applicable.

Appendix A. Matrix theorems

Theorem 1. *If Λ is a diagonal matrix in which all the elements λ_k are different, then to leading order in ε the eigenvalues of the matrix*

$$\Lambda + \varepsilon A$$

are: $\lambda_k + A_{kk}, k = 1, 2, \ldots$.

Proof. The proof is very simple [12]. Clearly, to leading order the eigenvalues are simply the λ_k. We write the kth eigenvalue as $\lambda_k + \varepsilon\lambda_k^{(1)}$ and substitute into the eigenvalue equation

$$\mathrm{Det}\left(\Lambda + \varepsilon A - I\left(\lambda_k + \varepsilon\lambda_k^{(1)}\right)\right) = 0. \tag{31}$$

Now divide the kth row by ε and let $\varepsilon \to 0$; we find that $\lambda_k^{(1)} = A_{kk}$. □

Theorem 2. *The matrix A has only diagonal elements, apart from rows p and q say which are general. Then the determinant of the matrix is $C(A_{pp}A_{qq} - A_{pq}A_{qp})$, where C is the product of the diagonal elements apart from those in rows p and q.*

Proof.

$$\mathrm{Det}\,(A) = \varepsilon_{i_1 i_2 \ldots i_p \ldots i_q \ldots i_n} a_{1i_1} a_{2i_2} \ldots a_{ni_n} = C\varepsilon_{123\ldots i_p \ldots i_q \ldots n} a_{pi_p} a_{qi_q} = C(a_{pp}a_{qq} - a_{pq}a_{qp}),$$

where $\varepsilon_{i_1 i_2 \ldots i_n}$ is the permutation symbol. □

Theorem 3. *If two of the diagonal elements say λ_p and λ_q of the matrix of Theorem* 1 *are equal, then the eigenvalues of the matrix*

$$\Lambda + \varepsilon A$$

are as before, except for those eigenvalues corresponding to rows p and q which are replaced by the eigenvalues of the matrix

$$\begin{bmatrix} A_{pp} & A_{pq} \\ A_{qp} & A_{qq} \end{bmatrix}.$$

Proof. Divide rows p and q of (31) by ε and then let $\varepsilon \to 0$. Theorem 2 then gives the required result. □

Appendix B. Zeros of H

The function H is defined by

$$H(\alpha) = \Omega^2 - \alpha^2 - \varepsilon\sqrt{\pi}\,\mathrm{e}^{-\alpha^2/4}.$$

When one sets $z = (\Omega^2 - \alpha^2)/4$ and $f(z) = H(\alpha)/4$, the problem reduces to showing that the function

$$f(z) = z - \varepsilon'\mathrm{e}^z, \quad \varepsilon' = \frac{1}{4}\varepsilon\sqrt{\pi}\,\mathrm{e}^{-\Omega^2/4},$$

has infinitely many zeros. Clearly the zeros must lie on the curve, $|z| = \varepsilon'|\mathrm{e}^z|$, and Fig. 9(a) shows this curve for various values of ε'. If $\varepsilon' > \mathrm{e}^{-1}$ the curve has a single branch; for $\varepsilon' < \mathrm{e}^{-1}$ it consists of two branches, one of which is a closed loop about the origin. Note that the slope of all curves tends to $\pm\infty$ as $y \to \pm\infty$. A point z on this curve is a zero provided it satisfies the further condition,

$$\mathrm{Arg}(z) = \mathrm{Arg}\left(\mathrm{e}^z\right) \quad \text{or} \quad \theta + 2n\pi = y, \tag{32}$$

where n is an integer. Fig. 9(b) shows graphs of the LHS of (32) for $n = 0, 1, \ldots$ and of the RHS in the case $\varepsilon' = 1$. The independent variable is taken to be $\tan^{-1}(x)$ so as to represent a semi-infinite range of x values on a finite interval. Clearly the graphs have infinitely many intersections, corresponding to infinitely many zeros of $f(z)$. For large n the zeros are given asymptotically by

$$y_n \approx \left(2n + \frac{1}{2}\right)\pi.$$

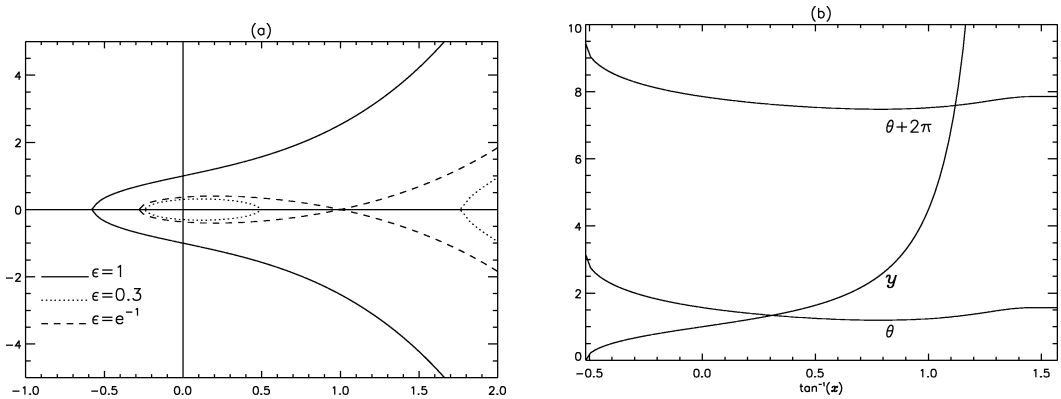

Fig. 9. (a) shows the curves $|z| = \varepsilon e^x$ for various values of ε. (b) shows graphs of $2n\pi + \theta$ and y versus x in the case $\varepsilon = 1$. The zeros of $f(z)$ correspond to the intersection points of the graphs.

References

[1] P.A. Davidson, An Introduction to Magnetohydrodynamics, Cambridge University Press, Cambridge, 2001.
[2] M. Faraday, Philos. Trans. (1831) 319.
[3] T.B. Benjamin, F. Ursell, The stability of the plane free surface of a liquid in vertical periodic motion, Proc. Roy. Soc. London 225 (1954) 505–515.
[4] N.W. McLachlan, Theory and Appplication of Mathieu Functions, Clarendon Press, Oxford, 1947.
[5] D. Triadis, The effects of viscosity on the Faraday instability for small amplitudes, Master thesis, University of Waikato, 2000.
[6] J.M. Galpin, Y. Fautrelle, Liquid-metal flows induced by low-frequency alternating magnetic fields, J. Fluid Mech. (1992).
[7] Y. Fautrelle, A.D. Sneyd, Magnetic stirring by low-frequency fields, J. Fluid Mech. (2001), in print.
[8] E.J. McHale, J.R. Melcher, Instability of a planar liquid layer in an alternating magnetic field, J. Fluid Mech. 114 (1982) 27–40.
[9] Deepak, J.W. Evans, The stability of an interface between viscous fluids subjected to a high-frequency magnetic field and consequences for electromagnetic casting, J. Fluid Mech. 287 (1995) 133–150.
[10] Y. Fautrelle, A.D. Sneyd, Instability of a plane conducting free surface submitted to an alternating magnetic field, J. Fluid Mech. (1997), submitted.
[11] V.A. Yakubovich, V.M. Starzhinskii, Linear Differential Equations with Periodic Coefficients, Vols. 1 and 2, Wiley, 1975.
[12] I.M. Gel'fand, V.B. Lidskii, On the structure of the regions of stability of linear canonical systems of differential equations, Amer. Math. Soc. Transl. Ser. 2, 8 (1958) 143–182.
[13] E.C. Titchmarsh, The Theory of Functions, Oxford University Press, Oxford, 1939. Section 3.4.
[14] M. Garnier, R. Moreau, Effect of finite conductivity on the inviscid stability of an interface submitted to a high frequency magnetic field, J. Fluid Mech. 127 (1983) 365–377.
[15] Y. Fautrelle, A.D. Sneyd, Instability of a plane conducting free surface submitted to an alternating magnetic field, J. Fluid Mech. 375 (1998) 65–83.
[16] D.W. Jordan, P. Smith, Nonlinear Ordinary Differential Equations, Oxford University Press, Oxford, 1987.